

Theoretical Study of Mixed Silicon–Lithium Clusters $\text{Si}_n\text{Li}_p^{(+)}$ ($n = 1–6$, $p = 1–2$)

C. Sporea, F. Rabilloud,* X. Cosson, A. R. Allouche, and M. Aubert-Frécon

Laboratoire de Spectrométrie Ionique et Moléculaire, UMR 5579 (Université Claude Bernard Lyon 1 and CNRS), 43 Boulevard du 11 Novembre 1918, 69622 Villeurbanne Cedex, France

Received: November 23, 2005; In Final Form: March 1, 2006

Theoretical study on the structures of neutral and singly charged $\text{Si}_n\text{Li}_p^{(+)}$ ($n = 1–6$, $p = 1–2$) clusters have been carried out in the framework of the density functional theory (DFT) with the B3LYP functional. The structures of the neutral Si_nLi_p and cationic Si_nLi_p^+ clusters are found to keep the frame of the corresponding Si_n , Li species being adsorbed at the surface. The localization of the lithium cation is not the same one as that of the neutral atom. The Li^+ ion is preferentially located on a Si atom, while the Li atom is preferentially attached at a bridge site. A clear parallelism between the structures of Si_nNa_p and those of Si_nLi_p appears. The population analysis show that the electronic structure of Si_nLi_p can be described as $\text{Si}_n^{p-} + p\text{Li}^+$ for the small sizes considered. Vertical and adiabatic ionization potentials, adsorption energies, as well as electric dipole moments and static dipolar polarizabilities, are calculated for each considered isomer of neutral species.

1. Introduction

The properties of small clusters of semiconductor elements present a significant interest from the point of view of chemical structure and bonding. They are expected to have physical and chemical properties different from those of the bulk material because of their physical size.

Small Si_n clusters have been intensively investigated both theoretically and experimentally. In particular, an enormous effort has been devoted to determining the structures of free silicon clusters. For small Si_n clusters, $n < 8$, structures have been extensively studied from theory and are now firmly established.¹ They have been confirmed experimentally by anion photoelectron spectroscopy² or by Raman³ and infrared⁴ measurements on matrix-isolated clusters. The situation is far from clear for larger clusters despite many efforts. The search for the global minima needs both accurate potential functions and an efficient optimization method. These conditions can be achieved for small sizes, but as the cluster size increases, it becomes much more difficult to find the lowest-energy ground state in theoretical study. The calculated lowest-energy structures were found to be dependent on the type of the calculation (semiempirical,⁵ tight-binding,⁶ diffusion Monte Carlo,⁷ density functional theory (DFT),^{1,8} mixed semiempirical + DFT,⁹ mixed tight-binding + DFT¹⁰) and also on the optimization technique. For cationic silicon clusters, mobility experiments¹¹ have revealed that a structural transition from prolate to a more spherical geometry occurs between $24 \leq n \leq 27$, while for neutral silicon clusters photoionization experiments¹² have shown that the prolate-to-spherical-like structural transition is likely between $20 \leq n \leq 22$.

Binary clusters containing silicon atoms have been substantially studied. Mixed transition metal silicon clusters have been the object of experimental studies by mass spectrometry¹³ or by photoelectron spectroscopy.¹⁴ On the theoretical point of view, the Si_nM_p clusters have usually been investigated in the framework of DFT. This approach allows calculation of some

properties, particularly the geometrical structures of large systems, for a reasonable computational effort. Very recently, Binning and Babelo¹⁵ have investigated the structures and energetics of Si_nBe_n and $\text{Si}_n\text{Be}_{2n}$ ($n = 1–4$) clusters while Zhang et al.¹⁶ have published an investigation of Si_nAg ($n = 1–5$) clusters. Majunder and Kulshreshtha¹⁷ have investigated impurity-doped Si_{10} clusters (Si_{10}M , $\text{M} = \text{Li}, \text{Be}, \text{B}, \text{C}, \text{Na}, \text{Mg}, \text{Al}$, and Si) showing that the location of the impurity atom on the host cluster depends on the atomic size and the nature of interaction between the host cluster and the impurity atoms. The principal question in studying metal-doped silicon clusters is the comprehension of the modifications of the properties compared to the case of bare silicon clusters.

The study of alkali–silicon clusters is also of significant interest. Alkali metals adsorbed on semiconductor surfaces have been extensively studied^{18–22} because they work as a promoter in catalysts. The study of alkali–silicon clusters could furnish a better understanding in the interaction between silicon and alkali atoms and could help to find the best sites of adsorption. Until now, only the sodium-doped silicon clusters have been investigated. The ionization potentials of Si_nNa_p , $3 \leq n \leq 11$, $1 \leq p \leq 4$, have been experimentally determined from the threshold energies of their ionization efficiency curves.²³ On the theoretical aspect, the structural and electronic properties of Si_nNa ($n \leq 10$) have been studied through calculations based on the Moller–Plesset (MP2–MP4) method²³ or in the framework of DFT.²⁴ It has been found that the ionization potential for Si_nNa clusters presents local minima for $n = 4, 7$, and 10 , correlating with the measured low values²⁵ of the electron affinity of bare silicon clusters Si_n for these sizes. In a previous work,²⁶ we have investigated the neutral Si_nNa_2 clusters and their cations Si_nNa_p^+ ($p = 1, 2$) with DFT/B3LYP type calculations. The geometrical structure of the most stable isomers of Si_nNa_2 clusters was found to be similar to that of Si_nNa in which a second Na atom is located on a site far from the first Na atom. No Na–Na bonding was found for these small sizes. Our ab initio calculations indicate that on doping with Na atoms, the electron charge migrates from sodium atoms to the silicon cluster without disturbing seriously the original

* Corresponding author. Phone: 33 4 72 43 29 31. Fax: 33 4 72 43 15 07. E-mail: franck.rabilloud@lasim.univ-lyon1.fr.

TABLE 1: Equilibrium Distances (R_e in Å) and Vertical Ionization Potentials (vIP in eV) for Si_2 , Li_2 , SiLi , and SiLi^+ Dimers

molecule	R_e				exptl
	MP2/6-311+G(d)	BPW91/6-31+G(d)	B3LYP/6-31+G(d)	B3LYP/6-311+G(d)	
Si_2 ($^3\Sigma_g^-$)	2.164	2.303	2.171	2.166	2.246 ^a
Li_2 ($^1\Sigma_g^+$)	2.747	2.771	2.725	2.705	2.673 ^a
SiLi^+ ($^1\Sigma^+$)	2.747	2.847	2.811	2.770	
SiLi ($^4\Sigma^-$)	2.362	2.410	2.391	2.369	
molecule	vIP				exptl
	MP2/6-311+G(d)	BPW91/6-31+G(d)	B3LYP/6-31+G(d)	B3LYP/6-311+G(d)	
Si_2 ($^3\Sigma_g^-$)	10.164	7.834	7.856	7.882	7.9 ^b
Li_2 ($^1\Sigma_g^+$)	4.335	5.133	5.254	5.322	5.113 ^c
SiLi ($^4\Sigma^-$)	4.987	6.747	6.449	6.647	

^a Ref 37. ^b Ref 38. ^c Ref 39.

framework of the silicon cluster. For all the Si_nNa_2 clusters, the 3s electrons of the two Na atoms are transferred to the LUMO (lowest unoccupied molecular orbital) of Si_n and the electronic structure of Si_nNa_2 clusters correspond approximately to that of $\text{Si}_n^{2-} + 2\text{Na}^+$.

In the present work, we have investigated the electronic and structural properties of neutral or cationic lithium-doped silicon clusters $\text{Si}_n\text{Li}_p^{(+)}$, $n \leq 6$, $p \leq 2$. It could be interesting to compare the properties of these clusters to those of Si_nNa_p . While lithium and sodium atoms have similar external electronic structure, species containing Li or Na present significant differences.²⁷ For example, some differences have been already observed concerning the optical absorption spectra of small clusters. On the other hand, several experimental results^{28–30} have shown that Li adsorption on a Si surface is quite different from those of the other alkali metals, because the small size of Li atoms leads to a higher ability to intermix and react with a Si surface. The study of lithium-doped silicon clusters could help to understand the nature of chemical bonding between Li and Si atoms.

Both neutral and singly charged species are investigated in the framework of DFT. To our knowledge, this work is the first investigation of $\text{Si}_n\text{Li}_p^{(+)}$ clusters. Details of the calculations are introduced in section 2. Results are presented in section 3, where the calculated properties of clusters including structures, charge transfer, adsorption energy, ionization potential, electric dipole moment, and static dipolar polarizability are discussed.

2. Computational Details

Calculations have been carried out by use of the computational chemistry program Gaussian98³¹ and the graphical interface Gabedit.³² They were achieved in the linear combination of atomic orbitals scheme. To select a calculation method, we have tested several methods and basis sets for known properties of Si_2 , Li_2 , SiLi , and SiLi^+ dimers. The first method tested was based on the second order of perturbation using a Moller–Plesset zero-order Hamiltonian (MP2).³³ This method is known to be very dependent on the basis set, but as we are interested in investigating clusters including tens of atoms the basis should not be too large. We have chosen the 6-311+G(d) basis set, which was 14s10p1d contracted into 7s6p1d on silicon and 12s6p1d contracted into 5s4p1d on lithium. The others tests were performed in the framework of DFT using the BPW91 functional which includes Becke’s 1988 exchange functional³⁴ with the correlation functional of Perdew and Wang³⁵ or the hybrid B3LYP functional which involves Becke’s three-parameter exchange functional.³⁶ Two basis sets were tested. The first one (6-31+G(d)) was 17s11p1d contracted into 5s4p1d on silicon and 11s5p1d contracted into 4s3p1d on lithium, while the second one was 6-311+G(d).

All results are given in Table 1 for dimers for both the equilibrium distance R_e and the vertical ionization potential (vIP). The MP2/6-311+G(d) calculations were found to give inaccurate results concerning the vIP. This might be due to the basis set, so for Si_2 we have tested others basis like 6-311+G(2df,p)³¹ and SDD³¹ but without any real improvement. We concluded that the electronic correlation needs a more sophisticated approach like the MP4 or QCISD⁴⁰ methods with a large basis and so heavy calculations. The two functionals tested with the DFT approach furnish results of the same accuracy and better than MP2 ones. In addition, a relative small basis set, like 6-31+G(d), was found to be sufficient to give good results. With B3LYP/6-31+G(d), the ground state of SiLi is found to be a $^4\Sigma^-$ with an equilibrium distance of 2.391 Å and a dissociation energy of 1.57 eV in very good agreement with the QCISD(T) values of Boldyrev et al.⁴¹ A $^2\Pi$ excited state is found to be located 0.34 eV above the $^4\Sigma^-$ ground state with an equilibrium distance of 2.579 Å. For SiLi^+ , the ground state is found to be $^1\Sigma^+$ with an equilibrium distance of 2.811 Å and a dissociation energy of 0.75 eV into $\text{Si} + \text{Li}^+$, also in very good agreement with the QCISD(T) values of Boldyrev et al.⁴¹ A good compromise between accuracy and computational resources was obtained for B3LYP/6-31+G(d) calculations which reproduce experimental values of R_e and vIP with a relative error less than 3% for both molecules Li_2 and Si_2 .

After these tests, we choose to perform calculations on clusters $\text{Si}_n\text{Li}_p^{(+)}$ in the DFT approach with the B3LYP functional and the 6-31+G(d) basis set. In the optimization process of cluster geometries, a number of structures were tested for each size. We have initiated the geometry optimization process of Si_nLi_p clusters from the known frame of the corresponding Si_n cluster on which lithium atoms were located either on Si atoms or bridged over two atoms or capped on several atoms. We have also tested structures for which the frame of the corresponding Si_n cluster used as the initial geometry was deformed. We have also taken advantage of the known structures of Si_nNa_p .²⁶ Of course, the explicit treatment of all the electrons in a cluster having a large number of atoms constitutes a demanding computational task, and the search for the lowest isomer cannot include a global optimization procedure of the potential energy surface. So we cannot be sure that a more stable cluster than those found in our calculations does not exist. All optimizations were carried on without symmetry constraints (C_1 symmetry group). The stability of Si_nLi_p structures so obtained was examined by evaluating the harmonic frequencies. In the discussion we only report on the lowest-energy stable isomers determined in our optimizations. For each stable structure, the charges on the Li atoms have been estimated through a natural population analysis (NPA).⁴² Furthermore, the dipole moment

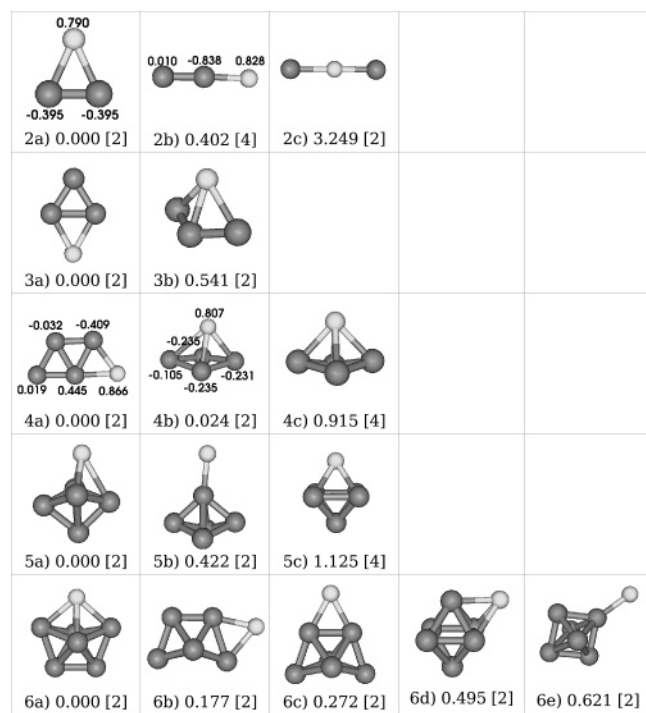


Figure 1. Optimized geometries of neutral Si_nLi clusters. The relative energies (eV) and the spin multiplicities (in square brackets) are shown under the structure of each isomer. Charges from the natural population analysis (q_{NPA}) are indicated for structures 2a, 2b, 4a, and 4b.

μ as well the averaged static dipolar polarizability $\alpha = (\alpha_{xx} + \alpha_{yy} + \alpha_{zz})/3$ have been calculated.

3. Results and Discussion

A. Lowest-Energy Structures and Isomers. The optimized geometries of the Si_nLi clusters, together with the energies of isomers relative to that of the lowest-energy one as well as the spin multiplicities, are shown in Figure 1. The ground state of all the Si_nLi ($n > 1$) clusters examined is a doublet. The structure of the most stable isomer keeps the frame of the corresponding Si_n unchanged. This means that the Si–Si bond predominates on the Si–Li one. The adsorbing site of a Li atom is a bridge-site type in which the Li atom is bridged over two Si atoms for $n = 2, 3$, and 4. The distance between Li and Si atoms in Si_2Li , Si_3Li , and Si_4Li clusters are found to be 2.588, 2.514, and 2.541 Å, respectively. The Si_3Li and Si_4Li structures are planar with a C_{2v} and C_s symmetry, respectively. For Si_4Li , the lowest-energy structure 4a is only slightly more stable than structure 4b by 0.024 eV, the latter being the lowest-energy isomer for Si_4Na .^{23,26} The Si_3Li and Si_6Li clusters present three-dimensional structures. For Si_5Li , the Li atom bridges over three Si atoms in structure 5a. The latter is 0.422 eV lower than the similar 5b structure in which Li is adsorbed on one Si atom. The adsorbing site of Li for Si_6Li is a bridge-site type in which the Li is capped over four Si atoms and with a distance between Li atom and Si atoms of 2.64 Å. This structure, which presents a C_{2v} symmetry, keeps unchanged the frame of the corresponding Si_6 cluster. There are still two others geometries constructed on the geometry of bare silicon cluster (structures 6b and 6c) in which the Li atom bridges over two Si atoms. As shown in Figure 1 the isomer 6a is below isomers 6b and 6c by 0.177 and 0.272 eV, respectively.

To check the structures and energetics, we have performed single-point calculations for trimers with the coupled cluster theory using the version involving single and double substitu-

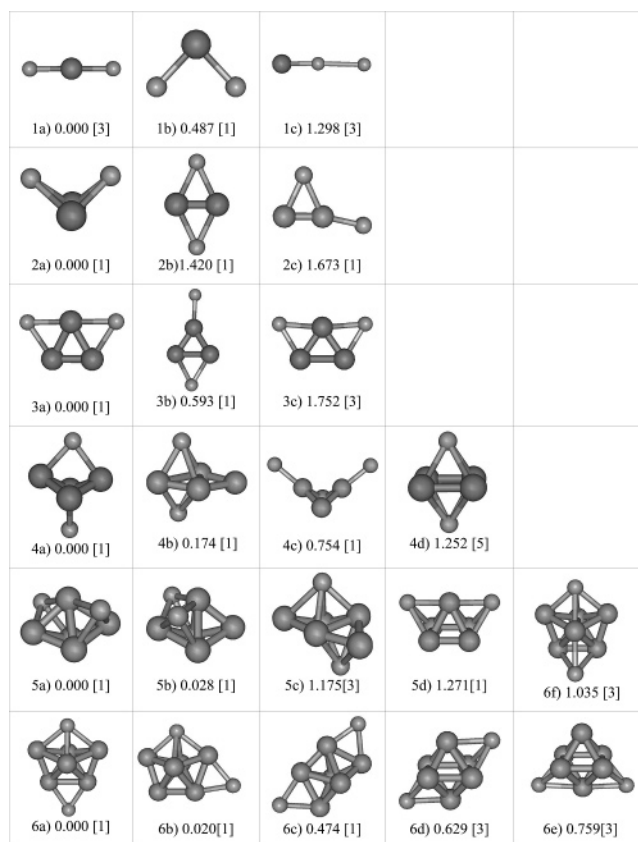


Figure 2. Optimized geometries of neutral Si_nLi_2 clusters. The relative energies (eV) and the spin multiplicities (in square brackets) are shown.

tions and taking into account the effect of the triple substitutions (CCSD(T)). We used the 6-31+G(d) basis set. We found that structure 3a is lower than 3b by 0.538 eV in perfect agreement with the 0.541 eV value of present B3LYP calculations.

The geometries of the Si_nLi_2 clusters as well as the spin multiplicities and relative energies for all isomers are shown in Figure 2. The ground state of Si_nLi_2 clusters is found to be a singlet, except in the case of SiLi_2 for which it is found to be a triplet. In the geometry optimization process, we have tested different positions for the second Li atom on the Si_nLi clusters surface. The geometrical structure of the most stable isomers is similar to that of Si_nLi (except for $n = 4$) in which a second Li atom is located on a site far from the first Li atom. The adsorbing site of the second Li atom is a bridge-site type in which the Li atom is bridged over two Si atoms for $n = 2, 3, 4$, and 6 or a bridge-site type in which the Li atom is capped over three Si atoms for $n = 5$. Si_2Li_2 and Si_3Li_2 present a C_{2v} symmetry. For Si_2Li_2 , the dihedral angle Li–Si–Li is 46.5° and all Si–Li bonds are found to be 2.53 Å. For Si_3Li_2 , the lowest-energy isomer is found to have a symmetric planar structure in which the Li atoms bridge a side of an isosceles triangle Si_3 . For Si_4Li_2 , isomer 4a is similar to isomer 4b of Si_4Li in which the Li atoms are located on both sides of the rhombus Si_4 . For $n = 5$ and 6, two quasi-degenerated structures (a and b) are in competition for the ground state.

The optimized geometries of the singly charged Si_nLi^+ clusters, together with the energies of isomers relative to that of the lowest-energy one as well as the spin multiplicities, are shown in Figure 3. The ground state is found to be a singlet for all sizes except for $n = 2$ for which it is found to be a triplet. The electronic structure of Si_nLi^+ can be described as $\text{Si}_n + \text{Li}^+$. The localization of the lithium ion is not the same one as that of the neutral atom in Si_nLi . For the lowest-energy isomer,

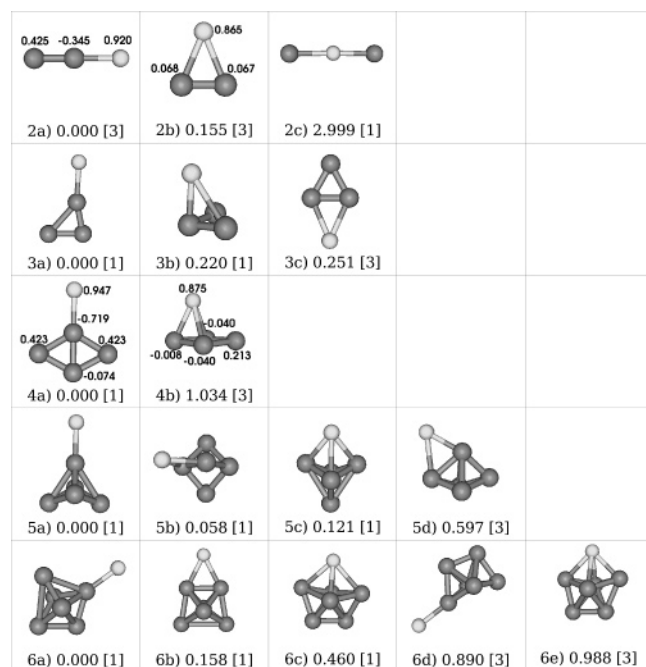


Figure 3. Optimized geometries of cationic Si_nLi^+ clusters. The relative energies (eV) and the spin multiplicities (in square brackets) are shown. Charges from the natural population analysis (q_{NPA}) are indicated for structures 2a, 2b, 4a, and 4b.

the Li^+ ion is located on a Si atom for all sizes. In this configuration the Li^+ charge generates an induced dipole in the globally neutral system Si_n (see Figure 3, isomers 2a and 4a). On the contrary, if the Li^+ bridges over two or more silicon atoms, it does not generate an induced dipole as shown in the Figure 3 in the cases of Si_2Li^+ and Si_4Li^+ . Thus, the Li^+ ion tends to bind over one silicon atom to minimize the interaction energy. The cation Si_2Li^+ has a nonsymmetrical linear structure with a Si–Li distance of 2.61 Å. The triangle structure is located 0.155 eV above. For the Si_3Li^+ cluster, the most stable isomer is planar, with a Li^+ tail and an irregular triangle Si_3 for which the length of the Si–Si bonds are found to be 2.76, 2.13, and 2.23 Å, respectively. Si_4Li^+ presents a C_{2v} symmetry with a Li^+ tail on one Si at 2.89 Å. For this size only one structure for singlet multiplicity was found to be stable. In the latter, the Li^+ cation is located on one Si atom of a rhombus Si_4 . The structure where the Li^+ capped the rhombus was found not to be stable as well as the structure where the Li^+ bridged two Si atoms. Si_5Li^+ has a C_{2v} symmetry. The Si–Li distance for $n = 4, 5,$ and 6 is found to be 2.56 Å for ground-state configurations.

To check the relative order in energy of isomers, we have performed single-point CCSD(T)/6-31+G(d) calculations for $n = 3$ and 4. Structure 3a was found to be more stable than structure 3b by 0.205 eV, and structure 4a was found to be more stable than structure 4b by 0.929 eV. These results are in very good agreement with the 0.220 and 1.034 eV values for $n = 3$ and 4, respectively, found with B3LYP.

The geometries of the singly charged Si_nLi_2^+ clusters, together with the relative energies of isomers and spin multiplicities, are shown in Figure 4. The ground state of all the Si_nLi_2^+ clusters examined is a doublet. The electronic structure is similar to that of $\text{Si}_n^- + 2\text{Li}^+$. The structures are approximately similar for both Si_nLi_2^+ and Si_nLi_2 clusters for $n = 1, 2,$ and $5,$ but are different for $n = 3, 4,$ and $6.$ For Si_nLi_2^+ clusters, Li atoms are located on a Si atom or bridges over two, three, or four Si atoms. As for neutral Si_nLi_2 clusters, the second Li atom is located on a site far from the first one. For Si_3Li_2^+ and Si_5Li_2^+ , isomers a

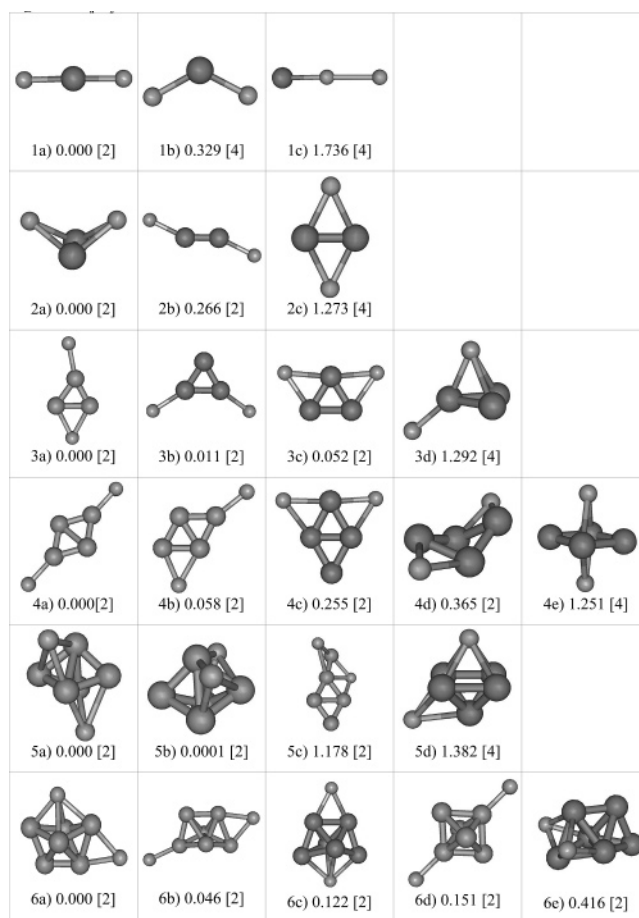


Figure 4. Optimized geometries of cationic Si_nLi_2^+ clusters. The relative energies (eV) and the spin multiplicities (in square brackets) are shown.

and b are found to be quasi-degenerated. SiLi_2^+ has the same linear geometry as SiLi_2 , but the Si–Li bond distance increases from 2.53 to 2.73 Å. Si_3Li_2^+ present a C_s symmetry.

The structures of $\text{Si}_n\text{Li}_p^{(+)}$ clusters considered in the present study can be compared with those of $\text{Si}_n\text{Na}_p^{(+)}$ clusters.²⁶ In all cases, the structure of the most stable isomer keeps the frame of the corresponding Si_n unchanged or slightly deformed, the Li or Na atoms being adsorbed at the surface. Most of the isomers are similar for the adsorption of Li or Na atoms, but the relative order in energy is sometimes changed. Several structures are found stable for one alkali and not stable for the other one.

B. Population Analysis. In our calculations, we have considered the natural population analysis (NPA), and the results are displayed in Tables 2 and 3. For all the Si_nLi clusters investigated here ($n \leq 6$), the valence electron 2s of the Li atom is transferred to the LUMO of Si_n , and the electronic structure of Si_nLi clusters corresponds to that of $\text{Si}_n^- + \text{Li}^+$. The natural population analysis indicates a charge q_{NPA} of about +0.8 on the Li atom (Table 2). These results are in concordance with the values obtained for Si_nNa ²⁶ (see Figure 5). In the Figure 1, the q_{NPA} charges for Si atoms are indicated for isomers a and b of Si_2Li and Si_4Li . They show that the transferred charge is located on the nearest neighbors. In the case of Si_2Li , one can see that the structure is most stable when the transferred electron can be shared by two silicons rather than located on only one silicon. For all the Si_nLi_2 clusters, the 2s electron of the two Li atoms are transferred to the LUMO of Si_n , and the electronic structure of Si_nLi_2 clusters corresponds approximately to

TABLE 2: Calculated Relative Energies, Lithium Binding Energies (E_b), Dipole Moments (μ), Static Dipolar Polarizabilities (α), and Charges on Lithium Atoms from the Natural Population Analysis (q_{NPA}) for Si_nLi Clusters

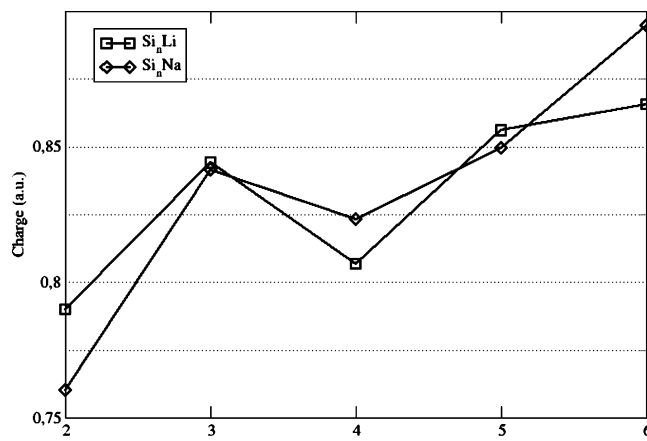
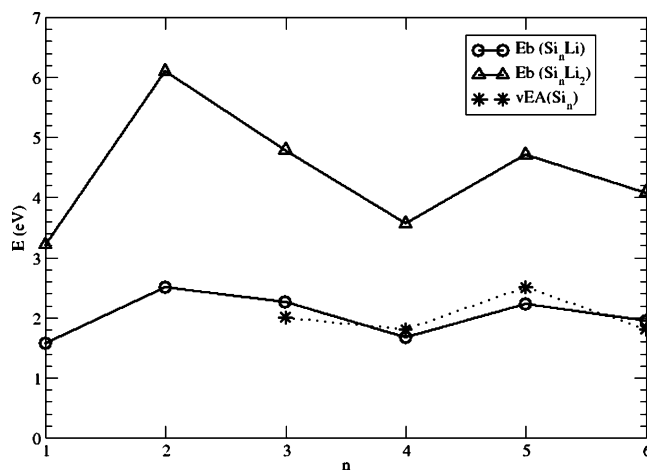
cluster	energy (eV)	E_b (eV)	μ (Debye)	α (\AA^3)	q_{NPA} (au)	
SiLi	0.000	1.57	5.98	11.19	0.78	
Si ₂ Li	2a (C_{2v})	0.000	2.50	5.62	19.71	0.79
	2b ($C_{\infty v}$)	0.402		4.73	18.41	
	2c ($C_{\infty v}$)	3.249		1.87	31.18	
Si ₃ Li	3a (C_{2v})	0.000	2.25	5.80	18.83	0.84
	3b (C_1)	0.541		4.40	21.01	
Si ₄ Li	4a (C_s)	0.000	1.67	6.89	24.56	0.81
	4b (C_s)	0.024		4.66	23.43	
	4c (C_s)	0.915		4.54	23.66	
Si ₅ Li	5a (C_s)	0.000	2.23	5.23	26.82	0.86
	5b (C_{2v})	0.422		9.74	28.69	
	5c (C_{4v})	1.125		3.54	25.94	
Si ₆ Li	6a (C_{2v})	0.000	1.95	4.44	30.08	0.87
	6b (C_s)	0.177		7.34	31.58	
	6c (C_{2v})	0.272		7.14	31.61	
	6d (C_s)	0.495		5.97	30.37	
	6e (C_{2v})	0.621		11.05	33.04	

TABLE 3: Calculated Relative Energies, Lithium Binding Energies (E_b), Dipole Moments (μ), Static Polarizabilities (α), and Charges on Lithium Atoms from the Natural Population Analysis (q_{NPA}) for Si_nLi_2 Clusters

cluster	energy (eV)	E_b (eV)	μ (Debye)	α (\AA^3)	q_{NPA} (au)	
SiLi ₂	1a ($C_{\infty v}$)	0.000	3.21	0.00	23.38	0.77; 0.74
	1b (C_{2v})	0.487		5.44	26.49	
	1c ($C_{\infty v}$)	1.298		10.15	31.49	
Si ₂ Li ₂	2a (C_{2v})	0.000	6.10	6.09	20.65	0.74; 0.74
	2b (D_{2h})	1.420		0.00	20.69	
	2c (C_s)	1.673		8.41	23.80	
Si ₃ Li ₂	3a (C_{2v})	0.000	4.78	5.21	23.74	0.85; 0.85
	3b (C_{2v})	0.593		3.78	26.00	
	3c (C_{2v})	1.752		6.49	27.88	
Si ₄ Li ₂	4a (C_s)	0.00	3.56	0.00	26.35	0.86; 0.86
	4b (C_s)	0.174		2.35	27.39	
	4c (C_{2v})	0.754		10.18	35.89	
	4d (C_1)	1.252		0.00	27.29	
Si ₅ Li ₂	5a (C_1)	0.000	4.70	4.31	29.79	0.86; 0.86
	5b (C_1)	0.028		5.98	29.91	
	5c (C_1)	1.175		1.06	31.30	
	5d (C_{2v})	1.271		5.16	32.35	
Si ₆ Li ₂	6a (C_{2v})	0.000	4.08	2.38	33.95	0.86; 0.89
	6b (C_s)	0.020		6.74	34.62	
	6c (C_{2v})	0.474		3.67	36.37	
	6d (D_{3d})	0.629		0.00	33.90	
	6e (C_{2v})	0.759		5.94	34.40	
	6f (C_s)	1.035		3.79	34.66	

that of $\text{Si}_n^{2-} + 2\text{Li}^+$. The natural population analysis indicates a charge q_{NPA} within the 0.7–0.9 range on each Li atom (Table 3).

C. Lithium Binding Energies. The binding energy of Li to the Si_n cluster for neutral species calculated as $E_b = -[E(\text{Si}_n\text{Li}_p) - E(\text{Si}_n) - pE(\text{Li})]$ is listed in Tables 2 and 3 for the most stable isomer of each size. In all cases, Li atoms are stably adsorbed on the Si_n frame. The evolution of E_b against the number of silicon atoms is shown in Figure 6. E_b oscillates as a function of n , showing a local minimum for $n = 4$ and local maxima for $n = 2$ and 5. This result is in concordance with the values²⁶ obtained for Si_nNa and is explained by the parallelism between E_b and the electron affinity of Si_n due to the fact that the binding of an alkali atom to the Si_n cluster

**Figure 5.** Charge (in au) on the alkali atom in Si_nLi clusters and Si_nNa clusters (ref 26) from the natural population analysis.**Figure 6.** Binding energy (E_b) of lithium atoms to the Si_n cluster for Si_nLi and Si_nLi_2 clusters, together with the experimental value of the vertical electron affinities (vEA) of Si_n (ref 25).

leads to an electronic charge transfer from the alkali atom to Si_n . The binding energy of two Li atoms is approximately equal to twice the binding energy of one Li atom. Our calculations show that alkali binding energy is higher for Si_nLi_p than for Si_nNa_p by an amount of 0.5–2.0 eV.

D. Ionization Potential. We now discuss the ionization potentials for Si_nLi_p clusters. We have calculated both the vertical ionization potential vIP (when the ion geometry is considered as identical to the geometry of the neutral) and the adiabatic ionization potential aIP (including the relaxation of the ion geometry) for Si_nLi and Si_nLi_2 clusters.

Before discussing results for clusters, we first present results for dimers. The vIP for Si_2 and Li_2 dimers are compared with the experimental values in Table 1. The B3LYP/6-31+G(d) values compared very well with the experimental data. For the SiLi dimer, the value of 6.449 eV for the vIP compared very well with the aIP of 6.45 eV obtained by Boldyrev et al.⁴¹ with the MP4/6-311+G(2df) and QCISD(T)/6-311+G(2df) methods. This overall agreement ascertains the reliability of the computational method applied in this work.

Results for Si_nLi and Si_nLi_2 clusters are displayed in Figures 7 and 8, respectively. For Si_nLi , the evolution of IPs against n presents a local minimum for $n = 4$ and two local maxima for $n = 3$ and 5, similar to previous results for Si_nNa .^{23,26} The evolution is similar to that of the electron affinity of Si_n , the latter giving a minimum for $n = 4$ and a maximum for $n = 5$ (Figure 6). This parallelism had already been noticed by Kishi

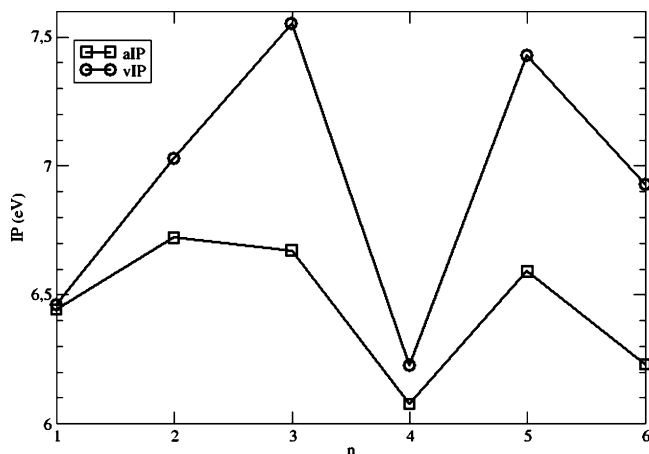


Figure 7. Calculated vertical (circle) and adiabatic (square) ionization potentials for Si_nLi clusters.

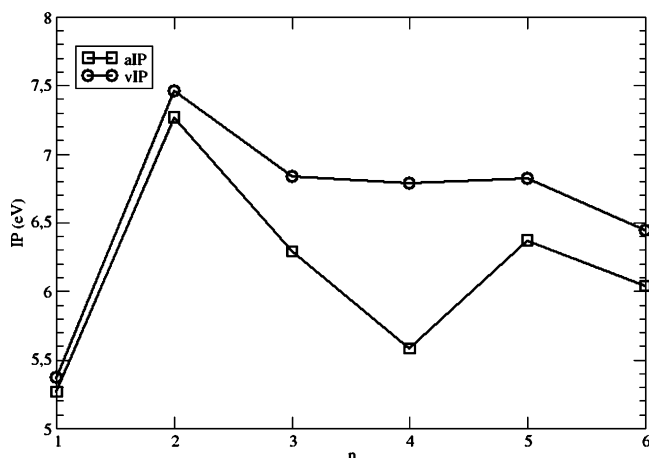


Figure 8. Calculated vertical (circle) and adiabatic (square) ionization potentials for Si_nLi_2 clusters.

et al.²³ and can be easily understood as the HOMO of Si_nLi is the LUMO of Si_n . The IPs for the lithium-doped cluster are significantly lower (1–1.5 eV) than those for the parent Si_n clusters.²⁴ The decrease reflects the change in the orbital being ionized, which is in Si_nLi of similar character as the LUMO of the parent Si_n . For Si_nLi_2 , the evolution is not exactly the same than for Si_nNa_2 ,²⁶ due to the fact that the isomers are not identical for both alkalis. For the two species, Si_nM and Si_nM_2 , the IPs for lithium-doped clusters are higher than those for sodium-doped ones by about 0.5 eV.

E. Dipole Moments and Polarizabilities. Dipole moments and static dipolar polarizabilities are two properties which could in principle make possible discrimination between different isomers. The dipole moments are interesting observables since they probe the charge distribution. We have calculated the dipole moments for all stable isomers. The results are shown in Table 2 for Si_nLi and Table 3 for Si_nLi_2 . For Si_nLi clusters, the transfer of one electron from the Li atom to the silicon cluster leads to a dipole moment μ . It has a value within the 4.44–6.89 D range for the most stable isomer of Si_nLi , and it is oriented from the center of mass of the silicon atoms toward the lithium atom. For Si_nLi_2 clusters, the dipole moment depends on the relative position of the two Li atoms. The symmetric structures (isomers 1a, 2b, 4a, 4d, and 6d) have a zero dipole moment. The calculated averaged static dipolar polarizabilities, $\alpha = (\alpha_{xx} + \alpha_{yy} + \alpha_{zz})/3$, are also given in Tables 2 and 3. The values increase with the size of the cluster, but generally for one given

size they are similar for the various isomers so that they do not furnish a discrimination between isomers.

4. Conclusions

We have performed a detailed study on the adsorption of one or two Li atoms in Si_n clusters with n ranging from 1 to 6. Calculations have been carried out for both neutral and singly charged clusters at the B3LYP/6-31+G(d) level. The structure of Si_nLi_p keeps the frame of the corresponding Si_n cluster unchanged, and the electronic structure of Si_nLi_p corresponds approximately to that of $\text{Si}_n^{p-} + p\text{Li}^+$. The localization of the lithium cation is not the same as that of the neutral atom. Li^+ ion is preferentially located on one Si atom while Li atom is preferentially attached at a bridge site. The Li^+ ion tends to bind over one silicon atom to minimize the interaction energy in generating an induced dipole in the globally neutral system Si_n , while for the neutral system the structure is more stable when the transferred charge can be shared by several silicon neighbors. The geometrical structure of the most stable isomers of Si_nLi_2 clusters was found to be similar to that of Si_nLi in which the second Li atom is located on a site far from the first Li atom. For all clusters studied here, the spin multiplicity of the lowest-energy isomer is found to be the lowest one for each size (doublet for Si_nLi and Si_nLi_2^+ , singlet for Si_nLi_2 and Si_nLi^+). A clear parallelism between the structures of Si_nNa_p and those of Si_nLi_p appeared. Vertical and adiabatic ionization potentials have been calculated as well as the dipole moments and static dipolar polarizabilities. Values of dipole moments are tightly connected to geometrical structures. To our knowledge, the present work is the first theoretical investigation of neutral and positively charged $\text{Si}_n\text{Li}_p^{(+)}$ clusters. We hope that our theoretical predictions will provide strong motivation for further experimental studies of these important silicon clusters and their cations.

References and Notes

- (1) Yang, J.; Xu, W.; Xiao, W. *J. Mol. Struct.: THEOCHEM* **2005**, *719*, 89 and references therein.
- (2) Arnold, C. C.; Neumark, D. M. *J. Chem. Phys.* **1993**, *99*, 3353.
- (3) Honea, E. C.; Ogura, A.; Murray, C. A.; Raghavachari, K.; Sprenger, W. O.; Jarrold, M. F.; Brown, W. L. *Nature* **1993**, *366*, 42.
- (4) Li, S.; Van Zee, R. J.; Weltner, W., Jr.; Raghavachari, K. *Chem. Phys. Lett.* **1995**, *243*, 275.
- (5) Yoo, S.; Zeng, X. C. *J. Chem. Phys.* **2003**, *119*, 1442.
- (6) Marin, L. R.; Lemes, M. R.; Dal Pino, A., Jr. *J. Mol. Struct.: THEOCHEM* **2003**, *663*, 159.
- (7) Grossman, J. C.; Mitos, L. *Phys. Rev. Lett.* **1995**, *74*, 1323.
- (8) Nigam, S.; Majumder, C.; Kulshreshtha, S. K. *J. Chem. Phys.* **2004**, *121*, 7756.
- (9) Tekin, A.; Hartke, B. *Phys. Chem. Chem. Phys.* **2004**, *6*, 503.
- (10) Rata, I.; Shvartsburg, A. A.; Horoi, M.; Frauenheim, T.; Siu, K. W.; Jackson, K. A. *Phys. Rev. Lett.* **2000**, *85*, 546.
- (11) Jarrold, M. F.; Constant, V. A. *Phys. Rev. Lett.* **1991**, *67*, 2994.
- (12) Fuke, K.; Tsukamoto, K.; Misaizu, F.; Sanekata, M. *J. Chem. Phys.* **1993**, *99*, 7807.
- (13) Beck, S. M. *J. Chem. Phys.* **1990**, *90*, 6306.
- (14) Ohara, M.; Koyasu, K.; Nakajima, A.; Kaya, K. *Chem. Phys. Lett.* **2003**, *371*, 490.
- (15) Binning, R. C., Jr.; Bacelo, D. E. *J. Phys. Chem. A* **2005**, *109*, 754.
- (16) Zhang, P. F.; Han, J. G.; Pu, Q. R. *J. Mol. Struct.: THEOCHEM* **2003**, *635*, 25.
- (17) Majumder, C.; Kulshreshtha, S. K. *Phys. Rev. B* **2004**, *70*, 245426.
- (18) Glander, G. S.; Webb, M. B. *Surf. Sci.* **1989**, *222*, 64.
- (19) Souda, R.; Hayami, W.; Aizawa, T.; Otani, S.; Ishizawa, Y. *Phys. Rev. Lett.* **1992**, *69*, 192.
- (20) Namiki, A.; Suzuki, S.; Kato, H.; Babasaki, Y.; Tanaka, M.; Nakamura, T.; Suzuki, T. *J. Chem. Phys.* **1992**, *97*, 3781 and references therein.
- (21) Bonzel, H. P.; Ertl, G. *Physics and Chemistry of Alkali Adsorption*; Elsevier: Amsterdam, 1989.
- (22) Batra, I. P. *Phys. Rev. B* **1989**, *39*, 3919.

- (23) Kishi, R.; Iwata, S.; Nakajima, A.; Kaya, K. *J. Chem. Phys.* **1997**, *107*, 3056.
- (24) Wei, S.; Barnett, R. N.; Landman, U. *Phys. Rev. B* **1997**, *55*, 7935.
- (25) Cheshnovsky, O.; Yang, S. H.; Pettiette, C. L.; Craycraft, M. J.; Liu, Y.; Smalley, R. E. *Chem. Phys. Lett.* **1987**, *138*, 119.
- (26) Sporea, C.; Rabilloud, F.; Allouche, A. R.; Frécon, M. *J. Phys. Chem. A* **2006**, *110*, 1046.
- (27) Benichou, E.; Allouche, A. R.; Aubert-Frécon, M.; Antoine, R.; Broyer, M.; Dugourd, P.; Rayane, D. *Chem. Phys. Lett.* **1998**, *290*, 171 and references therein.
- (28) Johansson, L. S. O.; Reihl, B. *Surf. Sci.* **1993**, *287/288*, 524.
- (29) Grehk, T. M.; Johansson, L. S. O.; Gray, S. M.; Johansson, M.; Flodström, A. S. *Phys. Rev. B* **1995**, *52*, 16593.
- (30) Chung, J. W.; Kim, C. Y.; Shin, K. S.; Lee, K. D. *Surf. Sci.* **1995**, *324*, 8.
- (31) Frisch, M. J.; Trucks, G. W.; Schlegel, H. B.; Scuseria, G. E.; Robb, M. A.; Cheeseman, J. R.; Zakrzewski, V. G.; Montgomery, J. A., Jr.; Stratmann, R. E.; Burant, J. C.; Dapprich, S.; Millam, J. M.; Daniels, A. D.; Kudin, K. N.; Strain, M. C.; Farkas, O.; Tomasi, J.; Barone, V.; Cossi, M.; Cammi, R.; Mennucci, B.; Pomelli, C.; Adamo, C.; Clifford, S.; Ochterski, J.; Petersson, G. A.; Ayala, P. Y.; Cui, Q.; Morokuma, K.; Malick, D. K.; Rabuck, A. D.; Raghavachari, K.; Foresman, J. B.; Cioslowski, J.; Ortiz, J. V.; Stefanov, B. B.; Liu, G.; Liashenko, A.; Piskorz, P.; Komaromi, I.; Gomperts, R.; Martin, R. L.; Fox, D. J.; Keith, T.; Al-Laham, M. A.; Peng, C. Y.; Nanayakkara, A.; Gonzalez, C.; Challacombe, M.; Gill, P. M. W.; Johnson, B.; Chen, W.; Wong, M. W.; Andres, J. L.; Gonzalez, C.; Head-Gordon, M.; Replogle, E. S.; Pople, J. A. *Gaussian 98*, revision A.6; Gaussian, Inc.: Pittsburgh, PA, 1998.
- (32) Gabedit is a graphical user interface for Gaussian, Molpro, Molcas, and MPQC ab initio programs available from <http://lasim.univ-lyon1.fr/allouche/gabedit>.
- (33) Moller, C.; Plesset, M. S. *Phys. Rev.* **1934**, *46*, 618.
- (34) Becke, A. D. *Phys. Rev. A* **1988**, *38*, 3098.
- (35) Perdew, J. P.; Wang, Y. *Phys. Rev. B* **1992**, *45*, 13244.
- (36) Becke, A. D. *J. Chem. Phys.* **1993**, *98*, 5648.
- (37) Huber, K. P.; Herzberg, G. Constants of Diatomic Molecules (data prepared by Gallagher, J. W.; Johnson, R. D., III.). In *NIST Chemistry WebBook*; Linstrom, P. J., Mallard, W. G., Eds.; NIST Standard Reference Database Number 69; National Institute of Standards and Technology: Gaithersburg, MD, 2005; 20899.
- (38) Winstead, C. B.; Paukstis, S. J.; Walters, J. L.; Gole, J. L. *J. Chem. Phys.* **1995**, *102*, 1877.
- (39) McGeogh, M. W.; Schlier, R. E. *Chem. Phys. Lett.* **1983**, *99*, 347.
- (40) Pople, J. A.; Head Gordon, M.; Raghavachari, K. *J. Chem. Phys.* **1987**, *87*, 5958.
- (41) Boldyrev, A. I.; Simons, J.; Schleyer, P. R. *J. Chem. Phys.* **1993**, *99*, 8793.
- (42) Reed, A. E.; Weinhold, F. *J. Chem. Phys.* **1983**, *78*, 4066.